Jpn. J. Appl. Phys. Vol. 36 (1997) pp. 165–169
Part 1, No. 1A, January 1997

Electron Energy-loss Spectroscopy Study of the Metal-insulator Transition in VO_2

Hiroyuki ABE, Masami TERAUCHI, Michiyoshi TANAKA, Shik SHIN[1] and Yutaka UEDA[2]

Research Institute for Scientific Measurements, Tohoku University, Sendai 980-77, Japan
[1]*Synchrotron Radiation Laboratory, Institute for Solid State Physics, The University of Tokyo, Tokyo 188, Japan*
[2]*Institute for Solid State Physics, The University of Tokyo, Tokyo 106, Japan*

(Received September 17, 1996; accepted for publication November 6, 1996)

Electron energy-loss spectra of VO_2 have been measured from perfect single crystalline areas of 100–180 nm diameter in the metallic and insulating phases. A sharp peak has been observed at 1.2 eV in the valence electron excitation spectra of the metallic phase but not in those of the insulating phase. We assign the peak to an interband transition or *d-d* transition by inspecting the dielectric function derived from the present loss function with the help of an energy band diagram already given, although an excitation at about 1 eV already observed by optical measurement was assigned to the excitation of a free-carrier plasmon. The peak due to the O 1*s* $\rightarrow$ V $3d(t_{2g})$ transition in the O 1*s* excitation spectra decreased in intensity but increased in the full width at half-maximum (FWHM) at the transition from the metallic phase to the insulating phase. These changes are considered to have been due to the fact that the $d_{//}$ band splits into the upper unoccupied and lower occupied $d_{//}$ bands and the upper $d_{//}$ band rises above the π^* band in the insulating phase, but that the $d_{//}$ band is unsplit and located within the π^* band in the metallic phase.

KEYWORDS: metal-insulator transition, EELS, free-carrier plasmon, interband transition

1. Introduction

It is known that VO_2, V_2O_3, V_6O_{13} and several Magnéli phases (V_nO_{2n-1}) undergo metal-insulator transitions (MIT) with a change of temperature.[1,2] Most of them are accompanied by crystal structure changes at the transition. Vanadium dioxide (VO_2) has a rutile structure with space group $P4_2/mnm$ in the metallic phase above 340 K and a monoclinic structure with space group $P2_1/c$ in the insulating phase below this temperature.[3,4] The fivefold degenerate V 3*d* levels split into triply degenerate lower t_{2g} levels and doubly degenerate upper e_g levels due to the cubic component of the octahedral crystal field. One of the t_{2g} orbitals, which points toward the orbital of the second nearest neighbor vanadium atoms, forms the $d_{//}$ band, and the other two t_{2g} orbitals form the π^* band as a result of hybridization with the O $2p\pi$ orbitals. These two bands almost overlap. The e_g orbitals form a broad σ^* band due to strong hybridization with the O $2p\sigma$ orbitals. The metallic behavior above 340 K is caused by the partial filling of the t_{2g} band, with one 3*d* electron per vanadium ion. The transition to the insulating phase is caused by splitting of the $d_{//}$ band into two bands and a rise of the π^* band above the Fermi level. The π^* band is located between the lower occupied $d_{//}$ band and the upper unoccupied $d_{//}$ band. The band gap energy in the insulating phase, which is the energy between the lower $d_{//}$ and π^* bands, was determined to be about 0.6 eV from optical measurements.[5] Goodenough[6] suggested that a driving force of the splitting is a lattice distortion. On the other hand, Zylbersztejn and Mott[7] argued the importance of an electron correlation for the splitting.

Changes in the electronic structure of VO_2 with the MIT were studied by optical measurements[5,8–12] and photoemission experiments.[11,13–17] Bianconi *et al.*[10] measured thermoreflectance spectra of VO_2 at the insulating and metallic phases, and observed a negative peak at 1.22 eV in the metallic phase (342 K) but not in the insulating phase. They identified the peak to be due to a free-carrier plasmon. The peak energy increased by 0.43 eV with the increase of temperature from 342 to 405 K. They considered that the absence of the free-carrier plasmon in the insulating phase was due to a zero electron density in the π^* band, and that the increase of the plasmon energy in the metallic phase with temperature was caused by an increase in electron density in the π^* band. The Hall-effect measurements conducted by Rosevear and Paul[18] did not show a change in carrier density in the metallic phase with temperature. This result is inconsistent with the interpretation of the temperature dependence by Bianconi *et al.*[10] Thus, the negative peak observed at 1.22 eV by Bianconi *et al.*[10] may not be caused by the free-carrier plasmon. Abbate *et al.*[12] measured X-ray absorption spectra of VO_2 at the metallic (393 K) and insulating (room temperature) phases with an energy resolution of 0.15 eV. They observed that the peak, which corresponds to the O 1*s* $\rightarrow$ V $3d(t_{2g})$ transition, separated into two peaks in the insulating phase. They assigned these peaks to the transitions into the $d_{//}$ and π^* bands. The peak intensity of the O 1*s* $\rightarrow$ V $3d(t_{2g})$ transition was smaller than that of the O 1*s* $\rightarrow$ V $3d(e_g)$ transition. X-ray absorption spectra measured by de Groot *et al.*[19] and Shin[20] and transmission electron energy-loss spectra measured by Lin *et al.*[21] did not show the separation in the insulating phase. These spectra showed that the peak intensity of the O 1*s* $\rightarrow$ V $3d(t_{2g})$ transition is larger than that of the O 1*s* $\rightarrow$ V $3d(e_g)$ transition, which was opposite to the observation reported by Abbate *et al.*[12] Since the unoccupied t_{2g} and e_g levels of VO_2 can accommodate five and four electrons, respectively, the peak intensity of the O 1*s* $\rightarrow$ V $3d(t_{2g})$ transition is expected to be higher than that of the O 1*s* $\rightarrow$ V $3d(e_g)$ transition. It is, therefore, a question of whether the result of Abbate *et al.*[12] is reliable.

The specimens used by Bianconi *et al.*[10] and Abbate *et al.*[12] are considered to contain oxygen deficiencies due to the escape of oxygen atoms from surfaces through irradiation of photons. Oxygen deficiencies cause an increase

in the number of carriers, resulting in an increase in the plasmon energy, and cause a decrease in the unoccupied density of states of the t_{2g} band, giving rise to a decrease in the peak intensity of the O $1s \rightarrow$ V $3d(t_{2g})$ transition. Specimens without oxygen deficiencies should be examined to allow detailed discussion of the change of electronic structures of VO_2 at the MIT. Transmission electron energy-loss spectroscopy (EELS) is not sensitive to the electronic states at surfaces but is used to measure electronic excitations in bulk crystals. This technique is therefore suitable for studying the electronic structures of bulk VO_2. We have measured the electron energy-loss spectra from perfect single crystalline areas of VO_2 using a high-resolution transmission EELS microscope to reveal the change of electronic structures at the MIT. The real ε_1 and the imaginary ε_2 part of the dielectric function are obtained from valence electron excitation spectra by Kramers-Kronig analysis and compared with the optical data. Core level excitation spectra are directly compared with X-ray absorption spectra because the intensity of these spectrta are proportional to ε_2.

2. Experimental

The high-resolution EELS microscope used was developed as a project of Joint Research with Industry by the Ministry of Education, Science, Sports and Culture.[22,23] The EELS microscope is equipped with a thermal-type field emission gun as the electron source and specially designed double-focus Wien filters as the monochromator and the analyzer. It incorporates an illumination lens system, a specimen goniometer and an imaging lens system of a JEM1200EX transmission electron microscope. Electron energy-loss spectra were taken by a parallel-recording system using a charge-coupled device (CCD) camera. The best values of the full width at half-maximum (FWHM) of the zero-loss peak are at present 15 meV without a specimen and 25 meV with a specimen. The energy of the incident electrons was set at 60 keV. The retarding potential of the monochromator was set to be 51 V and that of the analyzer was 200–520 V.

Single crystals of VO_2 were grown by the chemical vapor transport method using $TeCl_4$ as an agent material. Specimens for electron energy-loss spectra were prepared by crushing single crystals and fragments were placed on meshes for electron microscopy. Valence electron excitation spectra and core level excitation spectra were obtained from specimen areas of 100 and 180 nm diameter, respectively. The specimen areas were judged to be perfectly crystalline from their good electron diffraction patterns. The specimens were heated in a heating holder for electron microscopy. The temperature of the specimens was measured by a thermocouple near the specimens. The temperature difference between the specimens and the position of the thermocouple was estimated to be within ±10 K. The apparent temperature of the MIT was 350 K, instead of the reported value of 340 K.

3. Results and Discussion

3.1 *Valence electron excitation spectra*

Figure 1 shows electron energy-loss spectra of VO_2 measured at the insulating (300 K) and metallic (350 and 400 K) phases over an energy range of 0–60 eV with energy resolutions of 0.12, 0.16 and 0.15 eV for the FWHM of the zero-loss peak, respectively. The peak at about 4 eV is assigned to the interband transition from the O $2p$ band to the V $3d$ band.[11] The peak at about 10 eV is attributed to the interband plasmon due to the transition from the O $2p$ band to the V $4s$,$4p$ band.[11] The large peak at about 26 eV is due to the collective excitation of all valence electrons (valence plasmon). The valence plasmon energy was calculated to be about 20 eV in a free-electron approximation. The shift to the higher energy is caused by the strong transition from the O $2p$ band to the V $4s$,$4p$ band. The peaks at about 43 and 52 eV are assigned to the transitions from the V $3p_{3/2}$ and V $3p_{1/2}$ core levels to the V $3d$ band by referring to the electron energy-loss spectrum of vanadium metal.[24] The intensity ratio of the V $3p_{3/2}$ to V $3p_{1/2}$ excitations is different from that expected from the spin-orbit splitting (2 : 1). This is due to a strong interaction between the hole in the V $3p$ core level and the electron excited into the unoccupied V $3d$ band from the core level (core-hole interaction). Figure 2 shows electron energy-loss spectra of VO_2 measured at the insulating (300 K) and metallic (350 and 400 K) phases over an energy range of 0–5 eV with energy resolutions of 67, 65 and 68 meV for the FWHM of the zero-loss peak, respectively. Shoulders at 0.9 and 1.2 eV indicated by vertical lines are observed in the spectrum for the insulating phase (300 K). The peak at 1.2 eV indicated by an arrow appears upon the transition into the metallic phase (350 K). The peak energy is nearly the same as the free-carrier plasmon energy of 1.22 eV at 342 K reported by Bianconi *et al.*[10] The peak energy did not change with increasing temperature from

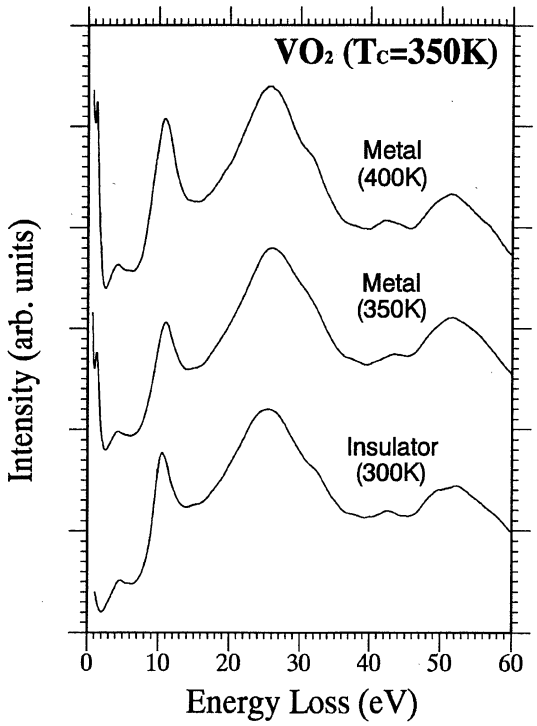

Fig. 1. Electron energy-loss spectra of VO_2 measured at the insulating (300 K) and metallic (350 and 400 K) phases over an energy range of 0–60 eV with energy resolutions of 0.12, 0.16 and 0.15 eV, respectively.

350 to 400 K, whereas Bianconi *et al.*[10] reported that the free-carrier plasmon energy increased by 0.43 eV with increasing temperature from 342 to 405 K.

The upper panels of Figs. 3(a) and 3(b) show the loss function ($\mathrm{Im}[-1/\varepsilon(\omega)]$) of the insulating (300 K) and metallic (350 K) phases, respectively, derived from Figs. 1 and 2. The contributions of the direct beam and multiple scattering were removed by a Lorentz fit and the Fourier-log deconvolution method,[25] respectively. The absolute value of the loss function was determined by applying $\mathrm{Re}[-1/\varepsilon(0)] \simeq -1/\varepsilon_1(0) = -1/n^2$ and $\mathrm{Re}[-1/\varepsilon(0)] = 0$ for the insulating and metallic phases, respectively. The refractive index n used for the insulating phase was 3.46, which was obtained by optical measurements.[5] The dielectric function was derived from the loss function by Kramers-Kronig analysis. The integration with energy in the analysis was carried out up to 400 eV, where a loss function above 60 eV was obtained by extrapolating the loss function using E^{-4} dependence.[26] The lower panels of Figs. 3(a) and (b) show the real (ε_1) and imaginary (ε_2) parts of the dielectric function of the insulating (300 K) and metallic (350 K) phases, respectively. Since ε_2 of the insulating phase (300 K) (Fig. 3(a)) has peaks at 1.0 and 1.2 eV, the peaks at 0.9 and 1.2 eV in the loss function, which correspond to the shoulders in the electron energy spectrum of Fig. 2, are due to interband transitions. Caruthers and Kleinman[27] calculated an energy band diagram of the insulating phase. They reported that the top of the occupied V 3*d* and the O 2*p* bands are located 0.6 and 1.8 eV below the bottom of the unoccupied V 3*d* band, respectively, and that of the unoccupied V 3*d* band is located 6.4 eV above the top of the occupied V 3*d* band. This is illustrated in Fig. 4(a). The minimum transition energy from the O 2*p* band to the unoccupied V 3*d* band is 1.8 eV and that from the occupied V 3*d* band to the V 4*s*,4*p* band is greater than 6.4 eV. Thus, the transitions at 0.9 and 1.2 eV are assigned to *d*–*d* transitions.

The condition for the plasmon excitation ($\varepsilon_1 = 0$) is

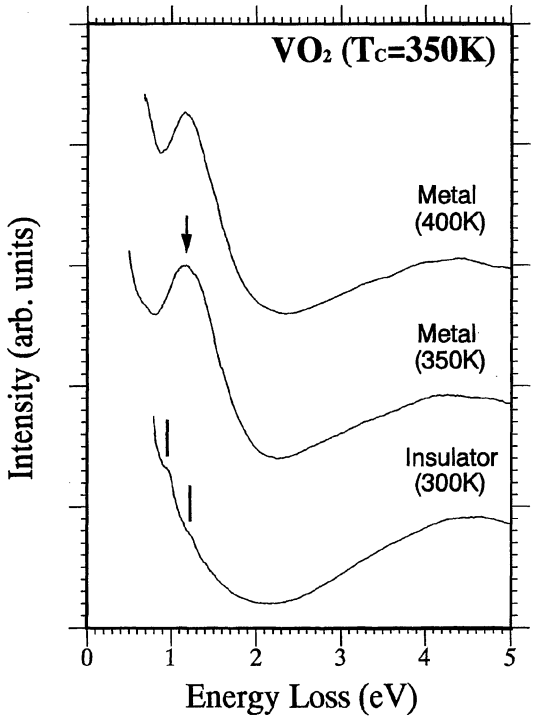

Fig. 2. Electron energy-loss spectra of VO_2 measured at the insulating (300 K) and metallic (350 and 400 K) phases over an energy range of 0–5 eV with energy resolutions of 67, 65 and 68 meV, respectively. The peak at 1.2 eV indicated by an arrow appears upon the transition into the metallic phase (350 K).

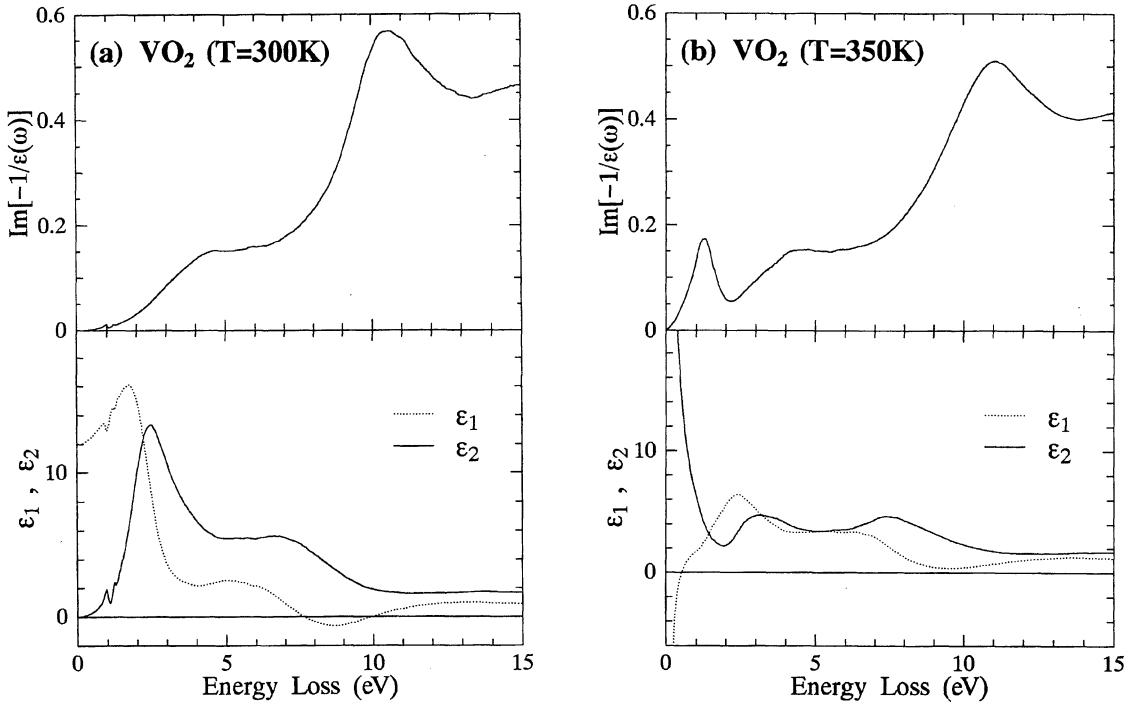

Fig. 3. The loss function ($\mathrm{Im}[-1/\varepsilon(\omega)]$), the real part ($\varepsilon_1$) and the imaginary part (ε_2) of the dielectric function of VO_2 at the insulating phase (300 K) (a) and the metallic phase (350 K) (b). The dielectric function was derived by Kramers-Kronig analysis of the loss function.

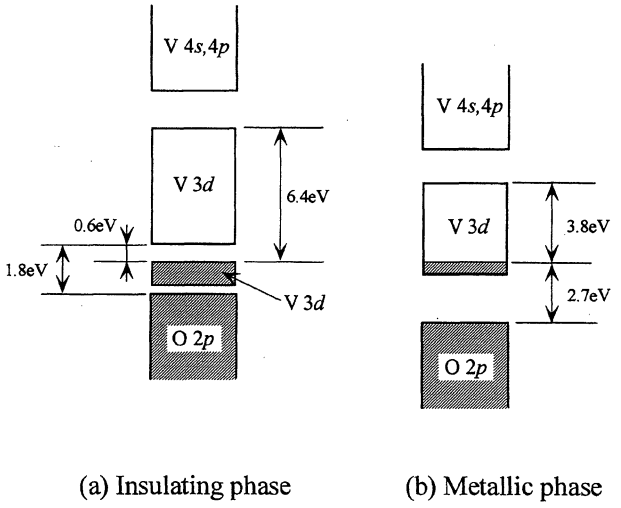

Fig. 4. Schematic energy bands of VO_2 at the insulating (a) and metallic (b) phases obtained from a calculation by Caruthers *et al.* (refs. 27 and 28)

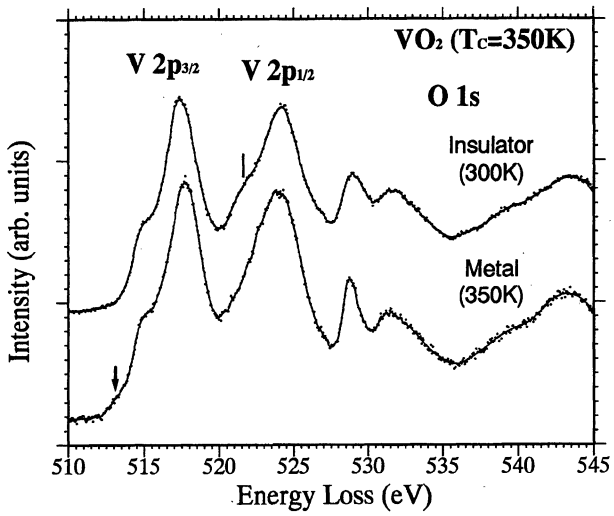

Fig. 5. Electron energy-loss spectra of VO_2 measured at the insulating (300 K) and metallic (350 K) phases over an energy range of 510–545 eV with an energy resolution of 0.24 eV.

satisfied at 0.6 eV in the metallic phase (350 K) (Fig. 3(b)). Thus, the plasmon excitation can arise at this energy but was not actually observed because of the strong damping of the plasmon due to the large value of ε_2, which originates from the interband and intraband transitions. Since ε_1 shows a non-zero value and a feature of a weak oscillator at 1.1 eV, although a peak or shoulder is difficult to see in ε_2, the peak at 1.2 eV in the loss function is assigned not to a plasmon but to an interband transition. Caruthers *et al.*[28] calculated an energy band diagram of the metallic phase. They reported that the top of the O 2*p* band is located 2.7 eV below the Fermi level and that of the V 3*d* band is located 3.8 eV above it. This is illustrated in Fig. 4(b). The minimum transition energy from the O 2*p* band to the unoccupied V 3*d* band is 2.7 eV and that from the occupied V 3*d* band to the V 4*s*,4*p* band is greater than 3.8 eV. Thus the peak at 1.2 eV in the loss function cannot be assigned to these transitions. The peak must be due to the *d*–*d* transition. The transition is allowed because the V 3*d* band has a *p*-like characteristic due to the overlap of the V 3*d* orbitals with the O 2*p* orbitals, though it is formally forbidden by the dipole selection rule. Since the hybridization of the V 3*d* with O 2*p* orbitals is stronger in the metallic phase than in the insulating phase, the *d*–*d* transition is expected to be stronger in the former phase than in the latter phase. The present experiment revealed that the peak at 1.2 eV in the loss function is not due to the free-carrier plasmon but is presumably due to the *d*–*d* transition.

3.2 *Core level excitation spectra*

Figure 5 shows the electron energy-loss spectra measured at the insulating (300 K) and metallic (350 K) phases over an energy range of 510–545 eV with an energy resolution of 0.24 eV for the FWHM of the zero-loss peak. The spectra below 527 eV are the V 2*p* excitation spectra and those above 527 eV are the O 1*s* excitation spectra. The peaks at about 517 and 524 eV are attributed to excitations from the V $2p_{3/2}$ and V $2p_{1/2}$ core levels, respectively. The peak energy of the V $2p_{3/2}$ excitation spectrum decreased by 0.4 eV but that of the V $2p_{1/2}$ excitation spectrum did not almost change at the transition from the metallic phase to the insulating phase. The shoulder at 513.1 eV indicated by an arrow disappeared but that at 521.6 eV indicated by a line appeared at the transition to the insulating phase. The experimental spectral intensity ratio of the V $2p_{3/2}$ to V $2p_{1/2}$ excitations is different from that expected from the spin-orbit splitting (2 : 1). Such a deviation has already been reported by Fink *et al.*[29] and analyzed by Zaanen *et al.*[30] in the 3*d* transition metals. This indicates that there exists a strong core-hole interaction between the hole in the V 2*p* core level and the electron excited into the unoccupied V 3*d* band from the core level. Theoretical calculations are needed to explain the V 2*p* excitation spectra in detail. On the other hand, the core-hole interaction between the hole in the O 1*s* core level and the electron excited into the unoccupied V 3*d* band from the core level is not strong because the overlap of the O 1*s* orbital with the V 3*d* orbitals is small compared to that of the V 2*p* orbitals with the V 3*d* orbitals. Thus the change of the unoccupied V 3*d* band at the MIT can be seen directly from the change of the O 1*s* excitation spectra. The peaks at about 529 and 531 eV are assigned to the transitions from the O 1*s* core level to the unoccupied V $3d(t_{2g})$ and V $3d(e_g)$ bands, respectively. These transitions are made possible by the admixture of the V 3*d* orbitals with the O 2*p* orbitals, although they are not the dipole allowed transition. The broad peak at about 543 eV is assigned to the transition from the O 1*s* core level to the V 4*s*,4*p* band. The peak intensity of the O 1*s* $\rightarrow$ V $3d(t_{2g})$ transition decreased but the FWHM of the peak increased at the transition from the metallic phase to the insulating phase. By referring to the change of the 3*d* band structure proposed by Goodenough,[6] these changes of the spectra at the transition are considered to be due to the fact that the $d_{//}$ band splits into the upper unoccupied and lower occupied $d_{//}$ bands, and that the upper $d_{//}$ band rises above the π^* band. Abbate *et al.*[12]

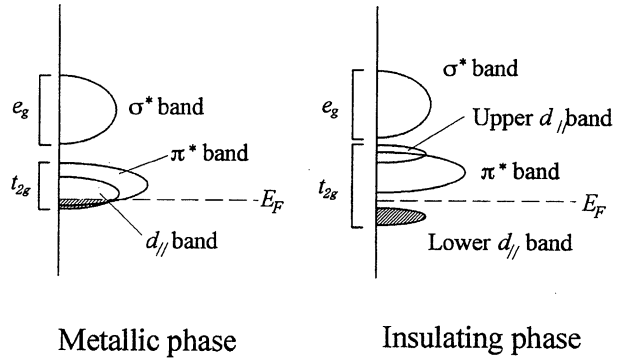

Fig. 6. Schematic energy diagrams of the V 3*d* band at the metallic and insulating phases. The unoccupied part is deduced from the results of the present experiment and the occupied one from the results of a photoemission experiment. (ref. 11)

reported that they observed a separation between the upper $d_{//}$ and π^* bands in the X-ray absorption spectra of the insulating phase with an energy resolution of 0.15 eV. However, we were not able to observe such a separation in electron energy-loss spectra taken at a higher energy resolution of 0.11 eV, which is not shown here. We consider that the energy difference between the two bands is not large enough for the peak of the O $1s \rightarrow$ V $3d(t_{2g})$ transition to separate into two peaks. The energy of the O $1s \rightarrow$ V $3d(e_g)$ transition increases by 0.2 eV at the transition from the metallic phase to the insulating phase without the change of the peak shape. The change of the V 3*d* bands at the MIT deduced from the present experiment is shown schematically in Fig. 6. The change of the O 1*s* excitation spectra at the transition from the metallic phase to the insulating phase indicated that the $d_{//}$ band splits into the upper unoccupied and lower occupied $d_{//}$ bands. The O 1*s* excitation spectrum of the insulating phase showed that the upper unoccupied $d_{//}$ band does not separate completely from the π^* band, although Abbate *et al.*[12] reported complete separation of the two bands.

4. Conclusion

We measured electron energy-loss spectra of VO_2 from perfect single crystalline areas of 100–180 nm diameter at the metallic and insulating phases. It was revealed that the peak at 1.2 eV in the loss function is due not to the free-carrier plasmon but to the *d*–*d* transition from the dielectric function obtained from the valence electron excitation spectra. It is noted that a similar misassignment was corrected by Terauchi *et al.*[26] in the case of the oxide superconductor $Bi_2Sr_2CaCu_2O_8$. The O 1*s* excitation spectra of the insulating phase showed that the $d_{//}$ band splits into the upper unoccupied and lower occupied $d_{//}$ bands and that the upper unoccupied $d_{//}$ band does not separate completely from the π^* band.

A similar substance of V_2O_3 also undergoes an MIT with a change of temperature. A free-carrier plasmon at about 1eV was detected by the optical measurement by Shuker and Yacoby.[31] It is worthwhile to reexamine the plasmon of V_2O_3 using EELS. The EELS study of the excitation at about 1 eV of V_2O_3 will be reported on elsewhere.

Acknowledgements

The authors would like to thank Dr. Y. Harada, Mr. M. Ishida and Dr. K. Tsuno of JEOL Ltd. for their great effort to construct the high-resolution EELS microscope. They would also like to thank Mr. F. Sato for his skillful technical assistance. The present work was partly supported by a Grant-in-Aid from the Ministry of Education, Science, Sports and Culture.

1) F. J. Morin: Phys. Rev. Lett. **3** (1959) 34.
2) S. Kachi, T. Takada and K. Kosuge: J. Phys. Soc. Jpn. **18** (1963) 1839.
3) G. Andersson: Acta Chem. Scand. **10** (1956) 623.
4) D. B. McWhan, M. Marezio, J. P. Remeika and P. D. Dernier: Phys. Rev. B **10** (1974) 490.
5) Hans W. Verleur, A. S. Barker, Jr. and C. N. Berglund: Phys. Rev. **172** (1968) 788.
6) J. B. Goodenough: J. Solid State Chem. **3** (1971) 490.
7) A. Zylbersztejn and N. F. Mott: Phys. Rev. B **11** (1975) 4383.
8) V. G. Mokerov and A. V. Rakov: Fiz. Tverd. Tela **11** (1969) 197. Translation: Sov. Phys.-Solid State **11** (1969) 150.
9) B. S. Borisov, S. T. Koretskaya, V. G. Mokerov, A. V. Rakov and S. G. Solov'ev: Fiz. Tverd. Tela **12** (1970) 2209. Translation: Sov. Phys.-Solid State **12** (1971) 1763.
10) A. Bianconi, S. Stizza and R. Bernardini: Phys. Rev. B **24** (1981) 4406.
11) S. Shin, S. Suga, M. Taniguchi, M. Fujisawa, H. Kanzaki, A. Fujimori, H. Daimon, Y. Ueda, K. Kosuge and S. Kachi: Phys. Rev. B **41** (1990) 4993.
12) M. Abbate, H. Pen, M. T. Czyżyk, F. M. F. de Groot, J. C. Fuggle, Y. J. Ma, C. T. Chen, F. Sette, A. Fujimori, Y. Ueda and K. Kosuge: J. Electron Spectros. Relat. Phenom. **62** (1993) 185.
13) R. J. Powell, C. N. Berglund and W. E. Spicer: Phys. Rev. **178** (1969) 1410.
14) C. Blaauw, F. Leenhouts, F. Van der Woude and G. A. Sawatzky: J. Phys. C **8** (1975) 459.
15) S. Vasudevan, M. S. Hegde and C. N. R. Rao: Solid State Commun. **27** (1978) 131.
16) G. A. Sawatzky and D. Post: Phys. Rev. B **20** (1979) 1546.
17) N. Beatham, I. L. Fragala, A. F. Orchard and G. Thornton: J. Chem. Soc. Faraday Trans. II **76** (1980) 929.
18) W. H. Rosevear and W. Paul: Phys. Rev. B **7** (1973) 2109.
19) F. M. F. de Groot, M. Grioni, J. C. Fuggle, J. Ghijsen, G. A. Sawatzky and H. Petersen: Phys. Rev. B **40** (1989) 5715.
20) S. Shin (private communication).
21) X. W. Lin, Y. Y. Wang, V. P. Dravid, P. M. Michalakos and M. C. Kung: Phys. Rev. B **47** (1993) 3477.
22) M. Terauchi, R. Kuzuo, F. Satoh, M. Tanaka, K. Tsuno and J. Ohyama: Microsc. Microanal. Microstruct. **2** (1991) 351.
23) M. Tanaka, M. Terauchi, R. Kuzuo, K. Tsuno, J. Ohyama and Y. Harada: *Proc. 50th Annu. Meet. Electron Microscopy Society of America,* eds. G. W. Beily, J. Bentley and J. A. Small (San Francisco Press, San Francisco, 1992) p. 940.
24) D. L. Misell and A. J. Atkins: Philos. Mag. **27** (1973) 95.
25) R. F. Egerton: *Electron Energy-Loss Spectroscopy in the Electron Microscope* (Plenum, New York, 1996).
26) M. Terauchi, M. Tanaka, T. Takahashi, H. Katayama-Yoshida, T. Mochiku and K. Kadowaki: Jpn. J. Appl. Phys. **34** (1995) L1524.
27) E. Caruthers and L. Kleinman: Phys. Rev. B **7** (1973) 3760.
28) E. Caruthers, L. Kleinman and H. I. Zhang: Phys. Rev. B **7** (1973) 3753.
29) J. Fink, Th. Müller-Heinzerling, B. Scheerer, W. Speier, F. U. Hillerecht, J. C. Fuggle, J. Zaanen and G. A. Sawatzky: Phys. Rev. B **32** (1985) 4889.
30) J. Zaanen, G. A. Sawatzky, J. Fink, W. Speier and J. C. Fuggle: Phys. Rev. B **32** (1985) 4905.
31) P. Shuker and Y. Yacoby: Phys. Rev. B **14** (1976) 2211.